Article

Innovative Cross-sectional Configurations for Low-Cost Bamboo Composite (LCBC) Structural Columns

Cameron Padfield , Ben Drury , Ghazaleh Soltanieh , Mona Rajabifard , Amir Mofidi *

Posted Date: 3 July 2024

doi: 10.20944/preprints202407.0293.v1

Keywords: Green construction materials; Sustainable construction; Bio-based construction materials; Low-Cost Bamboo Composites (LCBC); Bio-resins; Bamboo Composites; Numerical modelling; Bio-epoxy; Furan resin

Article

Innovative Cross-Sectional Configurations for Low-Cost Bamboo Composite (LCBC) Structural Columns

Cameron Padfield [1], Ben Drury [2], Ghazaleh Soltanieh [3], Mona Rajabifard [4] and Amir Mofidi [5,*]

[1] Structural Engineer at WSP; cameron.padfield@wsp.com
[2] Structural Engineer at Fairhurst; ben.drury@fairhurst.co.uk
[3] Postdoctoral Fellow at Brock University; ghazaleh.soltanieh@brocku.ca
[4] Research Assistant at Brock University; mona.rajabifard@brocku.ca
[5] Associate Professor at Brock University; amir.mofidi@brocku.ca
* Correspondence: amir.mofidi@brocku.ca

Abstract: This paper investigates the effect of innovative cross-sectional configurations on Low-Cost Bamboo Composite (LCBC) structural members. The study employs both experimental and numerical methods with different resin matrices and bamboo species. In this study, LCBC short columns are designed with different innovative cross-sectional configurations in an attempt to overcome the costly production processes of engineered bamboo. This approach uses bundles of bamboo, both in culm and strip forms. A compatible, environmentally responsible, and economically justifiable resin matrix is used to fabricate an LCBC member. The production of LCBC members does not necessitate highly advanced technology. This capability enables the production of LCBC members in custom-designed cross-sectional shapes and lengths. This study introduces the Russian doll (RD), Big Russian doll (BRD), Hawser (HAW), and Scrimber (SCR) cross-sectional configurations. Extra-large, large, medium, and small sizes of bamboo are employed. Synthetic Epoxy (EXP), a Bio-based Experimental soft filler (BE1), Bio-Epoxy (BE2), Furan-based (PF1) matrices are applied. Furthermore, Moso, Guadua, Madake, and Tali bamboo species are incorporated. The results of this study reveal that the most efficient cross-sectional configuration for compressive strength is the HAW configuration, closely followed by SCR configuration. LCBC members with bio-resins have shown excellent promise in competing in strength with those made with their synthetic counterparts. The theoretical and numerical modeling of the LCBC members showed excellent correlation with the experimental results which provides the capacity to design LCBC for engineering projects. The LCBC design can be further developed with more bamboo and less resin content.

Keywords: green construction materials; sustainable construction; bio-based construction materials; Low-Cost Bamboo Composites (LCBC); bio-resins; Bamboo Composites; numerical modelling; bio-epoxy; furan resin

1. Introduction

The construction industry is a significant contributor to the issue of global warming, accounting for 36% of energy use and 39% of CO2 emissions globally [1–4]. Carbon-intensive materials like concrete and steel contribute to about one-third of the construction industry's emissions [5,6]. Therefore, there is a clear need to develop construction materials and methods. These should offer the required mechanical properties while minimizing their environmental impact on a global scale [7,8]. Structural timbers are promising sustainable options. However, a high level of costly processing is required before structural use. Furthermore, the level of supply and time required for the natural production of wood are not keeping pace with demands [9–12].

Bamboo presents the potential to address such shortcomings and provide a viable option capable of having the impact required [13–16]. It holds significant potential due to its widespread availability in regions where high demands are expected [16–18]. Bamboo's role as a carbon sink

 doi:10.20944/preprints202407.0293.v1

could support the reduction of carbon in the environment and its biodegradability could reduce waste [18]. Compressive strength of the bamboo fibres can be two to four times greater than that in structural timbers whilst tensile strength is approximately three times greater than timber and is comparable to steel [19]. Several challenges that could hinder bamboo's popularity in construction, stem from its nature [20]. In its raw form, bamboo is vulnerable to its surrounding environment. A popular misconception is that bamboo is highly effective under seismic loading [21]. However, alternative studies suggest that bamboo as a sole element is in fact less impressive, possessing several brittle failure modes [21].

Recent advancements have been made in the investigation of the use of bamboo in composite with alternative materials to develop Low-Cost Bamboo Composites (LCBC) as structural load-bearing members [20]. This progressive approach is a commercially reasonable attempt to benefit from the advantageous mechanical properties of raw bamboo materials while improving the irregularities and flaws of bamboo by using bundles of bamboo, in both culm and strip forms, in a compatible, environmentally responsible, and economically justifiable resin matrix. The production of LCBC: 1) does not require highly advanced technology, which makes the production of LCBC possible in many developing countries; 2) does not require multifaceted and energy-intensive processes, which helps better serve the sustainable purpose of this approach; 3) and can be conducted without a production line, which makes in-situ fabrication of the LCBC possible, a similar approach to the production of reinforced concrete (RC) members in construction sites. The latter capability of the LCBC approach will make the production of the LCBC members possible in costume-designed cross-sectional shapes and member lengths parallel with the installation of steel-embedded connection plates in the LCBC members during the fabrication phase of the members. Similar to RC member production in the concrete industry, precast LCBC structural members can also be produced in bulk in standardized shapes and sizes in addition to the in-situ production of the LCBC members. As for other advanced composite materials, the chosen matrices for LCBC members are not designed to bear much of the load. In fact, the resin matrix binds the bamboo culms and strips together and distributes the load among them, which increases the structural reliability of the composite material. It also provides ductility and protects the fibres from surface damage [21]. While the LCBC approach adopts its versatile production process from the structural concrete production, the underlying composite mechanics correspond to advanced composites research. Finally, the development process requires vast knowledge of the raw components used in LCBC based on extensive bamboo and bio-based resin research. To this end, the development of LCBC is a clear case of multi-disciplinary forward-thinking and evolutionary research study to develop a novel, practical, economical, and sustainable solution for green construction. It should be noted that the construction industry is already comfortable with similar application approaches such as casting, pouring uncured concrete, and fabricating structural members in situ, in addition to using uncured resins such as epoxy for delicate flooring purposes. In this manner, pouring uncured resins in stay-in-place casts for the production of LCBC members may not be considered less practical than the abovementioned already-established in-situ production processes in construction.

Despite some investigation having been completed, the proposal of LCBC structural members remains in its very early stages [20]. The current study investigates novel LCBC columns using four bamboo species, Moso, Guadua, Madake, and Tali. Four different cross-sectional configurations are studied. The configurations include the Russian doll, Big Russian doll, Hawser, and Scrimber. Smaller bamboo culms and strips are located with four different configurations in stay-in-place giant bamboo casts before the matrix is poured. The chosen matrices are promising bio-based resin matrices, including bio-epoxy and Polyfurfuryl alcohol (PFA), that are compared with their most recognized synthetic counterpart, Bisphenol A diglycidyl ether (BADGE), known as epoxy. To this end, 17 tests were conducted on LCBC short columns with diameters between 82 to 124 mm with primary test parameters including the cross-sectional configuration, bamboo species, and resin matrix.

 doi:10.20944/preprints202407.0293.v1

2. Materials and Methods

2.1. Bamboo Species

The species selection for the investigation can be attributed to already established use within a construction context and their respective availability. These bamboo species were categorized into four different size categories: extra large, large, medium, and small with diameters in millimeters between 100 to 125, 80 to 100, 40 to 50, and 20 to 25, respectively.

Moso is capable of achieving large diameters up to 7 inches (178 mm). As such, it presents potential in its use as a stay-in-place cast for the purpose of this investigation. In this study, Moso in size categories extra-large and large is utilized with a maximum diameter of 124 mm, in addition to being used in small size category. Moso is known to be available in a variety of sizes. It presents the opportunity for its use as an internal element of the LCBC member. The compressive strength of the giant Moso tested in this study is reported elsewhere [23] equal to 69.9 MPa.

Guadua is recognized as the largest, strongest, and most practical bamboo for construction in South America [24]. Upon research, compressive strength values obtained for Guadua have been within the region of 56 MPa [25] which again presents promise for global adoption and implementation. The reported compressive strengths of Guadua bamboo match an average of 60.7 MPa used in this study [23]. The Tali species used in this study are in the large category with a reported compressive strength of 59.1 MPa [23]. Madake species is native to East Asia. Madake can reach up to 6 inches (152.4 mm) in diameter. However, the larger sizes were not available at the time of this research and could therefore not be used as a stay-in-place cast for the specimens in extra-large or large categories. However, the species' mid-size diameter (medium size category) does present its ability for use as one of the internal culms within the different configuration types. Not only does it provide the opportunity to be placed within larger, more external culms, but the space within Madake specimens is also adequate for even smaller bamboo specimens to be placed. The chosen Madake species in this study therefore presents clear potential for its use in combination with alternate bamboo species and specimens in LCBC members.

It should be noted that in this study, for extra-large, medium, and small size categories there are only one species of bamboo as follows respectively, Moso, Madake, and Moso. Only for the large size category which plays the role of the stay-in-place cast for the majority of the specimens in this study (15 out of 17), there is a variety of species in Moso, Guadua, and Tali.

2.2. Resin Matrices

Currently, 75% of epoxies in worldwide use are bisphenol-based, a reprotoxic compound that also reduces the ability to biodegrade [26]. Subsequently, bio-epoxies have begun to be pursued. Until now, the most promising bio-epoxy systems have between 28% to 43% carbon contents derived from biological sources and are thus biodegradable [27]. Most epoxy resins were produced from epichlorohydrin. In the case of bio-epoxy, epichlorohydrin is mostly derived from a sustainable resource of bio-based glycerin such as Epicerol [28]. Furan resins are 100% bio-based resins made of hemicellulose fraction of biomass wastes which have been investigated as a matrix for natural fibre composites [29]. Furan bio-resins are heat-, fire-, and chemical-resistant.

In this study, four different resins are considered. A commercially available synthetic epoxy with the market name Epolam 2017 is chosen as a benchmark to compare the behaviour of the chosen bio-based resins with their synthetic counterpart (Figure 1a). An experimental soft bio-based resin was also used in this study to act as the holder of the smaller bamboo in the stay-in-place giant bamboo cast with minimized mechanical contributions (Figure 1b). A commercially-available bio-epoxy marketed as One resin manufactured by Entropy was used as the chosen bio-epoxy (Figure 1c). An available furfural-based resin made by TransFuran called Biorez was chosen as the PFA-based resin in this study (Figure 1 d).

 doi:10.20944/preprints202407.0293.v1

Figure 1. Resin matrices used: a) Epolam 2017 Synthetic Epoxy (EPX); b) Experimental soft filler (BE1); c) Entropy Bio-Epoxy (BE2); and d) BioRez PFA-based resin (PF1).

The compressive properties of the selected resins were measured in the laboratory based on ASTM D695-15 [30]. In particular, the compressive strength of the tested specimens for the synthetic epoxy (EPX), bio-based soft filler (BE1), bio-epoxy resin (BE2), and PFA-based resin (PF1) were measured equal to 78.9 MPa, 320 kPa, 94.3 MPa, and 42.0 MPa, respectively. The strain at maximum compressive strength with a linear stress-strain relationship for EPX, BE1, BE2, and PF1 are reported as 0.040, 0.338, 0.063, 0.019. The failure modes of the tested resins are shown in Figure 2a-d.

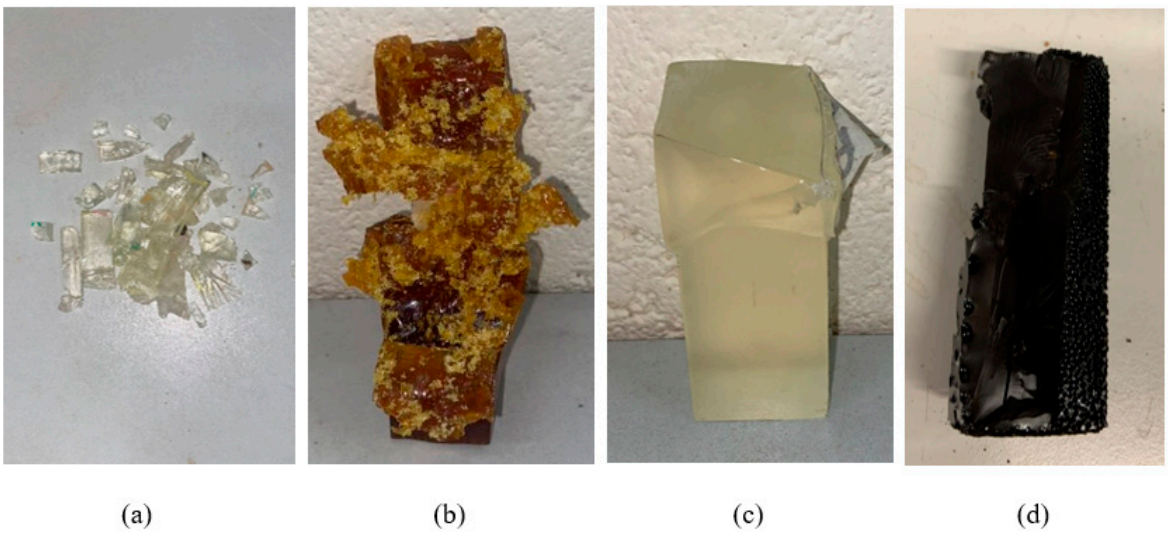

Figure 2. Failure modes of the studied resin matrices: a) Epolam 2017 Synthetic Epoxy (EPX); b) Experimental soft filler (BE1); c) Entropy Bio-Epoxy (BE2); and d) BioRez PFA-based (PF1) resin by TransFuran (PF1).

2.3. Cross-Sectional Configurations

The primary test parameter, in addition to the choices of bamboo species and resin matrices, concerns the cross-sectional configuration. In this investigation, a total of four different cross-sectional configurations were outlined and implemented.

The Russian Doll (RD) configuration is produced by the combination of three full culm bamboo specimens in different size categories (Figure 3a). Bamboo culms from large, medium, and small categories are placed within each other. The voids between bamboo culms are then filled by the resin

 doi:10.20944/preprints202407.0293.v1

component of the LCBC specimens. The Big Russian Doll (BRD) configuration is similar to that of the RD. However, the key difference between the two is that the BRD configuration consists of an extra full culm bamboo specimen taking the total full culms used in the composite to four (Figure 3b). Due to the larger number of culms in use, the external diameter of the LCBC member is larger than that of the RD composites. Similar to the RD series, different resins are used to fill the voids between each layer of BRD series. In the Hawser (HAW) configuration, five small category full culm bamboo specimens are placed within the stay-in-place large category bamboo culm before voids are filled by the resin component (Figure 3c). Scrimber (SCB) configuration differs from the other three configurations in that it is the only configuration in which split culm small bamboo is used. A large category full culm bamboo specimen is used as the stay-in-place cast for the SCB series. Several split small culm bamboo elements are then placed manually within the internal space of the cast before the resin is poured to fill the voids that remain (Figure 3d). It should be noted that the production of the scrimber series specimens is completely different from existing scrimber bamboo in the market. A major similarity is that both bamboo-based elements are made of split bamboo.

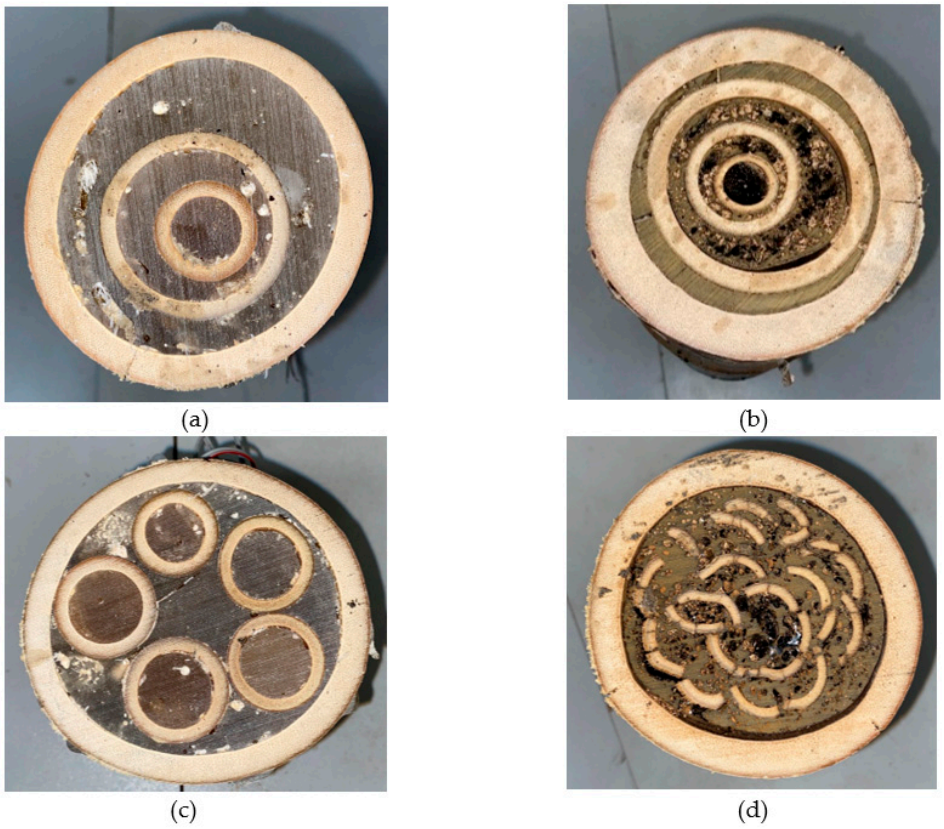

Figure 3. Cross-sectional configurations: a) Russian doll; b) Big Russian doll; c) Hawser; and d) Scrimber.

2.4. Labelling Conventions

Each test specimen was provided with a unique code for identification. The Moso, Guadua, and Tali species were coded as M, G, and T, respectively. When it comes to the cross-sectional configuration coding, BRD, RD, HAW, and SCR are chosen as discussed earlier. As for the used resin matrices, EPX is used for synthetic epoxy. BE1 is used for the soft filler matrix made from bio elements. BE2 was used for the commercial bio-epoxy marketed as One bio-epoxy by Entropy resins [31]. PF1 is the code for the PFA-based resin by TransFuran Chemicals [32]. In order to assess the reliability of the results, up to three specimens with similar test variables were produced and tested for certain specimens (the number of iterations after the species code, mainly M1 to M3). Table 1 provides information regarding the physical properties of all the LCBC specimens tested in this study with their corresponding specimen codes.

 doi:10.20944/preprints202407.0293.v1

Table 1. Physical properties of LCBC specimens.

Configuration	Specimen	D_{Outer} (mm)	Length (mm)	Mass (g)	Bamboo Content (%)	Resin Content (%)
Hawser (HAW)	HAW-EPX-M	96.3	96.9	649	41	59
	HAW-BE1-M	98.5	93.6	586	55	45
	HAW-BE2-M1	88.8	94.2	521	53	47
	HAW-BE2-M2	104.1	93.8	682	50	50
	HAW-BE2-M3	90.7	92.5	480	48	52
	HAW-PF1-M	88.5	99.7	347	52	48
Russian Doll (RD)	RD-EPX-M	98.7	97.6	679	43	57
	RD-BE1-G	82.9	87.0	422	47	53
	RD-BE2-M	93.2	92.8	545	49	51
	RD-BE2-T	84.7	98.3	406	54	42
	RD-BE2-G	80.6	95.2	424	49	44
	RD-PF1-M	100.9	128.5	792	56	41
	RD-PF1-T	82.7	99.6	330	48	52
Big Russian Doll (BRD)	BRD-BE2-M	119.8	93.5	819	59	41
	BRD-PF1-M	125.9	99.2	850	63	37
Scrimber (SCR)	SCR-BE2-M	91.3	100.0	513	56	44
	SCR-PF1-M	90.8	146.9	695	54	46

2.5. Experimental Testing Method

The chosen equipment to test and measure the compressive properties of LCBC specimens was a compressive testing machine with 8000 kN maximum loading capacity in compression. The bottom loading platen of the machine was equipped with a spherical bearing able to ensure the load was concentrically applied by allowing necessary rotations. The end planes of each specimen were adjusted with sandpaper to ensure the load transferred to the specimens uniformly (Figure 4). In addition, in between the loading platens and the specimen ends, an intermediate metallic sheet was added to minimize friction. The vertical load and displacement were automatically recorded by a computerized system at 1-second intervals. A loading rate 2.0 kN/s was utilized after a few trials to ensure failure of the specimens was reached within 300 ± 120 seconds, as per instructed by ISO 22157:2019 [22].

 doi:10.20944/preprints202407.0293.v1

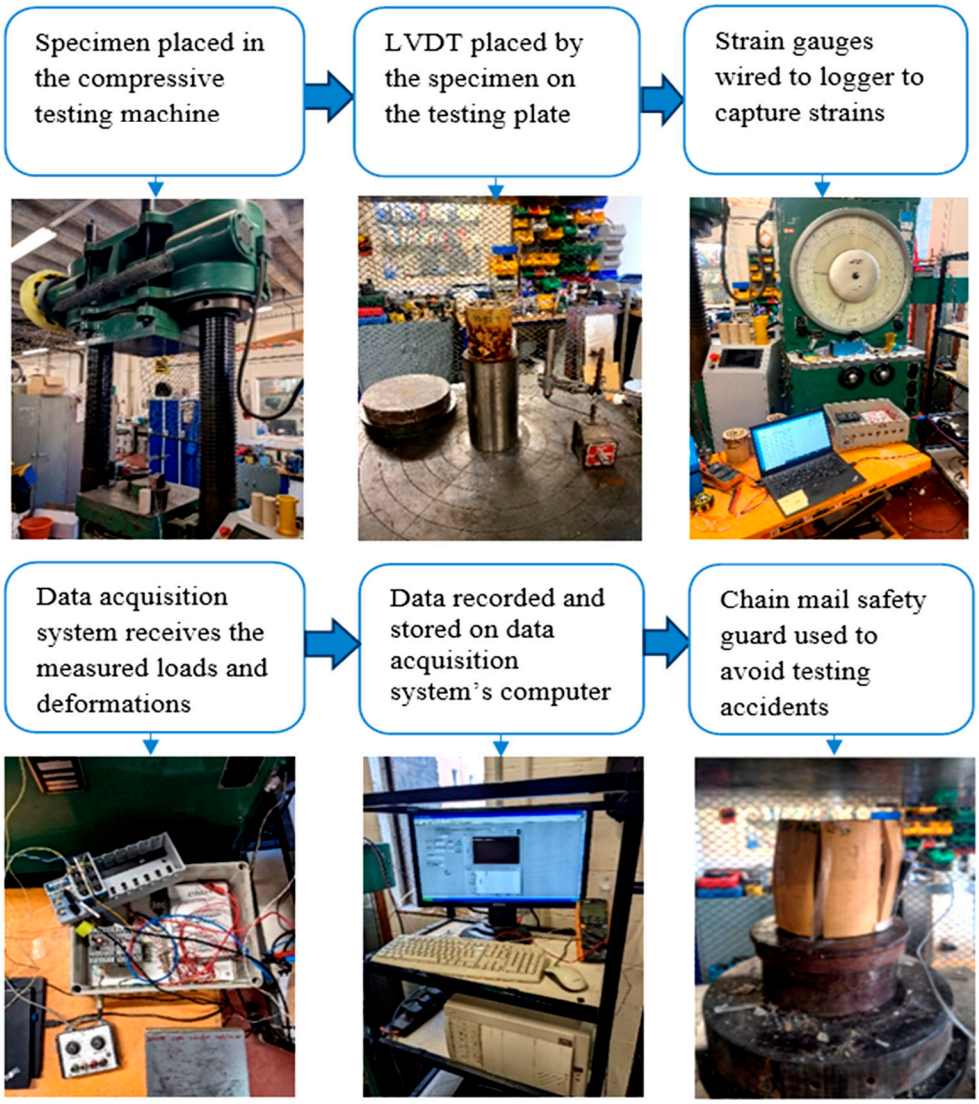

Figure 4. Experimental testing procedure on LCBC specimens.

The strain values are measured using strain gauges on the outer layer of the exterior bamboo (stay-in-place cast), while the longitudinal deformation is measured using Linear Variable Differential Transformers (LVDT).

3. Experimental Testing Results

In this investigation, 17 stocky LCBC columns were fabricated and tested. The principal test parameters in this study are: 1) the cross-sectional configuration of LCBC members; 2) resin matrices; and 3) the bamboo species. A full list of the produced LCBC members with their geometrical properties is shown in Table 1. The experimental results corresponding to the compression test of each specimen are presented in Table 2.

The results are presented in terms of the axial loads attained at the peak (Fult), the axial compressive stress reached at the peak (fc,0), the measured axial deformation at ultimate (ΔLc,0), the axial compressive strain reached the peak (c,0), and the modulus of elasticity of specimens in compression parallel to the fibres (Ec,0). In this section, the effects of different test parameters of the study are discussed based on the compression behaviours of the specimens in each category.

 doi:10.20944/preprints202407.0293.v1

Table 2. Experimental results of the compression tests.

Configuration	Specimen	$\Delta L_{c,0}$ (mm)	$\varepsilon_{c,0}$	F_{ult} (kN)	$f_{c,0}$ (MPa)	$E_{c,0}$ (GPa)
Hawser (HAW)	HAW-EPX-M	4.30	0.044	568	78	3.08
	HAW-BE1-M	3.76	0.038	220	36	1.32
	HAW-BE2-M1	3.37	0.035	398	64	3.89
	HAW-BE2-M2	4.23	0.043	567	67	2.54
	HAW-BE2-M3	4.48	0.049	363	56	2.01
	HAW-PF1-M	3.01	0.031	236	38	2.06
Russian Doll (RD)	RD-EPX-M	3.73	0.038	571	75	3.07
	RD-BE1-G	2.18	0.025	166	31	1.74
	RD-BE2-M	5.26	0.059	417	61	1.50
	RD-BE2-T	1.54	0.016	204	36	4.47
	RD-BE2-G	3.98	0.043	366	72	3.85
	RD-PF1-M	3.70	0.072	234	30	1.08
	RD-PF1-T	2.69	0.027	166	31	1.29
Big Russian Doll (BRD)	BRD-BE2-M	5.49	0.059	555	49	1.10
	BRD-PF1-M	4.28	0.043	500	40	1.18
Scrimber (SCR)	SCR-BE2-M	4.43	0.041	391	60	3.87
	SCR-PF1-M	5.54	0.038	225	35	1.39

3.1. Cross-Sectional Configuration Choice

3.1.1. Compressive Properties

Specimens produced with BE2 and PF1 resin matrices include all cross-sectional configurations proposed for the LBCB LCBC columns in this study. For these resin matrix series, only the specimens made with Moso bamboo were considered in this section to minimize the test parameter to the effect of cross-sectional configuration. The mechanical behaviour of the LCBC materials is compared here rather than the member behaviour for a fair comparison of the cross-sectional configurations.

Figure 5 presents the compressive stress versus the longitudinal strain in members made with all proposed configurations with BE2 resin and Moso bamboo.

It can be seen in Figure 5 that the specimens with HAW and SCR reach the greatest compressive strengths with 62 MPa and 60 MPa, respectively. The average strength of the three identical HAW specimens with 64 MPa, 67 MPa, and 56 MPa was used in this comparison. The configuration with the smallest compressive strength was the BRD with 49 MPa which can be attributed to the greater bamboo content in the cross-section versus resin content when compared to the other cross-sectional configurations (Table 1). The compressive strength of Moso bamboo used in this study, equal to 69.9 MPa reported in [23], is smaller than BE2 resin (94.3 MPa reported above). In addition, as discussed further, the bamboo component fails before the BE2 resin component when Moso bamboo and BE2 resin are used in an LCBC member. Therefore, a greater bamboo content in BRD configuration, compared to other configurations, had an adverse effect on the mechanical properties of the LCBC member. In this regard, the cross-sectional configurations with the stiffest compressive response were the SCR and HAW configurations with 3.87 GPa and 2.81 GPa moduli of elasticity (Table 2). As expected, the least stiff configuration was the BRD configuration due to higher bamboo content compared to other configurations.

 doi:10.20944/preprints202407.0293.v1

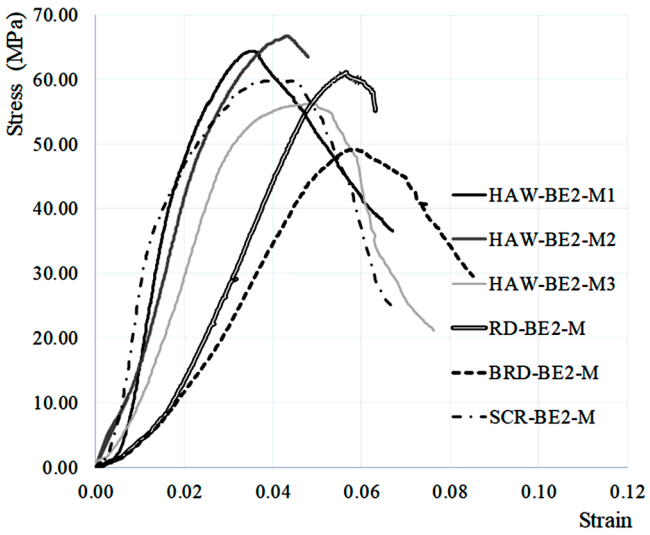

Figure 5. Compressive stress versus measured longitudinal strain of BE2 test series with different cross-sectional configurations.

The reported moduli of elasticity were calculated using the following equation (1) which is provided by ISO-22157:2019 [22].

$$E_{c,0} = \frac{F_{60} - F_{20}}{A(\varepsilon_{60} - \varepsilon_{20})} \quad (1)$$

The equation calculates the secant modulus of elasticity between the points corresponding to applied load and compressive strain of 60% and 20% of failure. In this manner, F_{60} and F_{20} are the applied load at 60% and 20% of the load at peak, correspondingly. Whereas ε_{60} and ε_{20} are the compressive strain corresponding to 60% and 20% of the load at peak, respectively.

Figure 6 illustrates the compressive behaviour of specimens with different cross-sectional categories made with PF1 resin matrix. As can be seen in Figure 6, the BRD, HAW, and SCR configurations reached the greatest compressive strengths of 40 MPa, 38 MPa, and 35 MPa, respectively (Table 2). As will be discussed later in the theoretical section of this article, the PF1 resin content fails ahead of Moso bamboo when PF1 resin and Moso bamboo are used together in an LCBC member. Here, the greater bamboo content of the BRD specimen (Table 1) has a favourable effect on the overall compressive behaviour of the LCBC member since the used Moso bamboo has a greater compressive strength than the PF1 resin (69.9 MPa versus 42.0 MPa, respectively). As for the compressive stiffness of the LCBC with different configurations, the HAW and SCR configurations presented the greatest moduli of elasticity with 2.06 GPa and 1.39 GPa, respectively.

After reviewing the behaviour of specimens in the BE2 and PF1 series containing specimens with all the proposed cross-sectional configurations, it appears that the most efficient cross-sectional configurations are the HAW and SCR configurations. The BRD, with higher than 60% bamboo content, is an efficient configuration when used with a resin equal to or less strong than bamboo in compression.

Preprints.org (www.preprints.org) | NOT PEER-REVIEWED | Posted: 3 July 2024 doi:10.20944/preprints202407.0293.v1

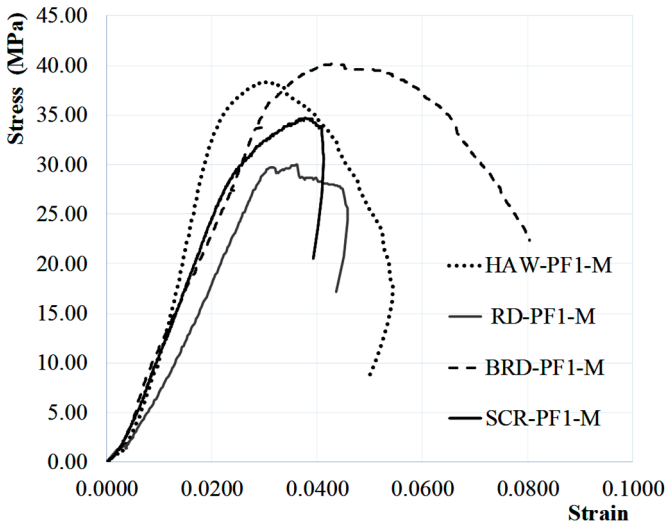

Figure 6. Compressive stress versus measured longitudinal strain of PF1 test series with different cross-sectional configurations.

3.1.2. Failure Modes

Figure 7a-g provide the failure modes of test specimens made with BE2 resin including specimens discussed above with different configuration types made with Moso bamboo.

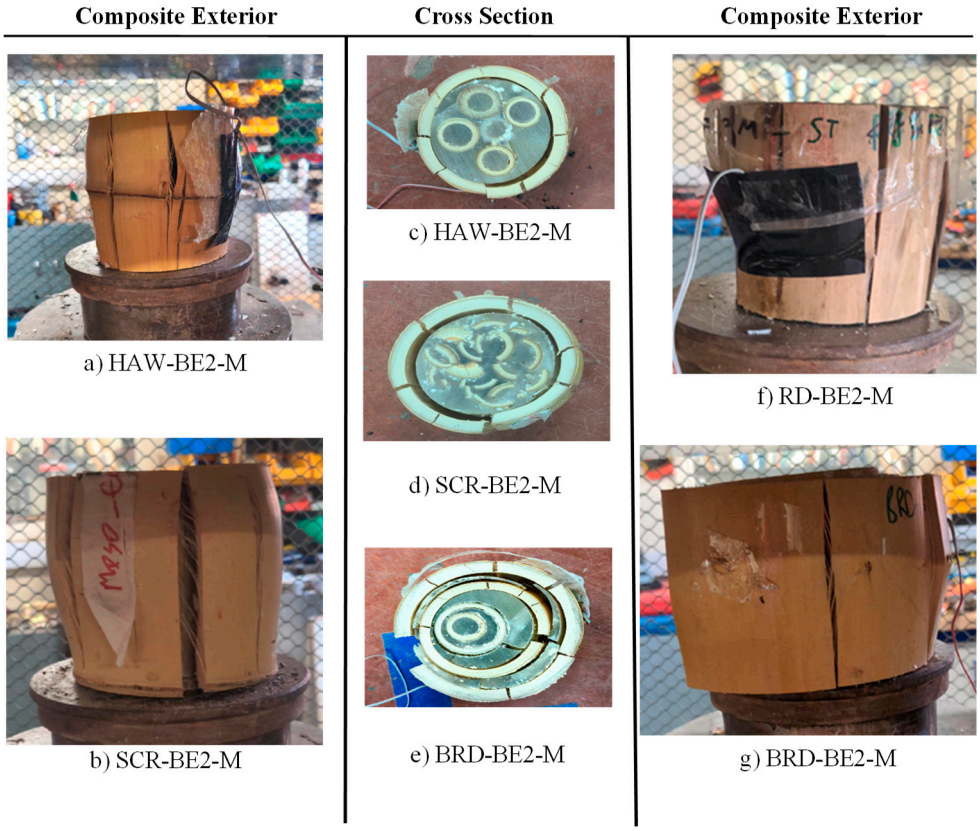

Figure 7. Effect of matrix configuration failure mode of LCBC specimens made with BE2 resin on failure mechanisms.

As can be seen in Figure 7, most specimens have suffered ultimate failures with longitudinal cracking across the outer layer of the cross-section. In all cases excluding the BRD sample (Figure 7e),

 doi:10.20944/preprints202407.0293.v1

the core matrix section appears undamaged after the ultimate which indicates a reserve capacity even after the ultimate failure due to the separation of the outer bamboo layer.

3.2. Resin Matrix Choice

3.2.1. Compressive Properties

The effect of the resin matrix used to produce the LCBC short columns can be observed when reviewing the compressive behaviour of HAW specimens made with Moso bamboo. Four different resins have been used to fabricate these specimens including EPX, BE1, BE2, and PF1. The compressive stress versus axial strain of all specimens with HAW configuration is presented in Figure 8.

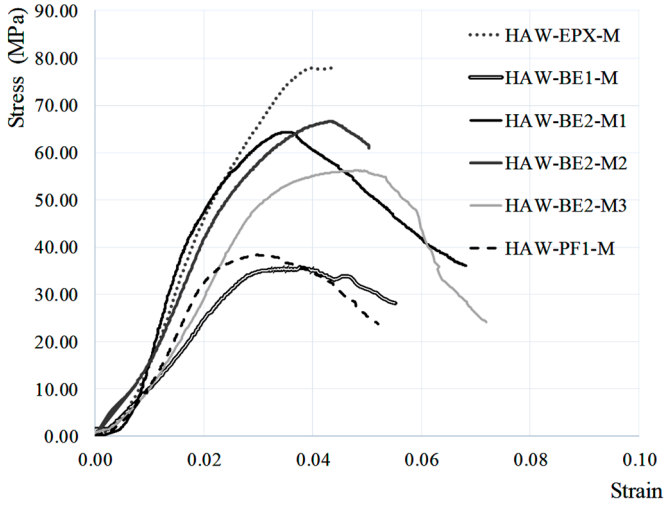

Figure 8. Compressive stress versus measured longitudinal strain of HAW test specimens with different resins.

The specimens made with synthetic epoxy (HAW-EPX-M) reached the greatest compressive strength (78 MPa) closely followed by the three specimens made with BE2 with 67 MPa, 64 MPa, and 56 MPa. It should be noted that the resin content of HAW-EPX-M was 59%, whereas the resin content of the specimens with bio-epoxy was 50% on average. While the configuration of all HAW specimens was the same with the same number of small bamboo within a large bamboo, the natural shape of the bamboo culms affected the total cross-sectional area of bamboo in each LCBC specimen, hence the differences in resin and bamboo contents. The specimen made with the soft resin (BE1) reached 36 MPa as the weakest specimen in compression. In terms of the moduli of elasticity of LCBC with different resin matrices, the stiffest specimens are HAW-BE2-M1, HAW-EPX-M, and HAW-BE2-M2 with 3.89 GPa, 3.08 GPa, and 2.54 GPa, respectively (Table 2). These are promising results with respect to the use of bio-epoxy instead of synthetic epoxy. Although the specimens made with PF1 did not contribute much to the compressive strength, the resin was able to add to the stiffness of the LCBC with the modulus of elasticity of 2.06 GPa when compared to the HAW-BE1-M specimen. The control specimen with soft resin (HAW-BE1-M) reached a modulus of elasticity of 1.32 GPa, mainly contributed by bamboo.

When reviewing the compressive behaviour of the specimens with different resins with RD configurations (Figure 9), similar results as those reported for the HAW specimens can be seen.

Figure 9 presents the compressive behaviour of specimens with resin matrices using Moso bamboo and RD configuration. As seen for the HAW series, the specimens made with synthetic epoxy (RD-EPX-M) reached the greatest compressive strength (75 MPa) closely followed by the specimen made with bio-epoxy with 72 MPa (Table 2). The specimen made with PF1 resin reached 30 MPa as the weakest specimen in compression. In term of the modulus of elasticity of LCBC with different

 doi:10.20944/preprints202407.0293.v1

resin matrices, the stiffest specimens are RD-EPX-M, RD-BE2-M, and RD-PF1-M with 3.07 GPa, 1.50 GPa, and 1.08 GPa, respectively (Table 2).

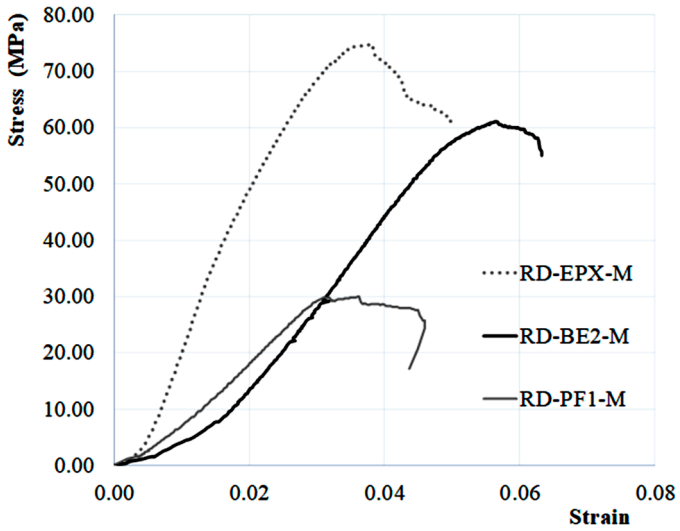

Figure 9. Compressive stress versus measured longitudinal strain of RD test specimens with different resins.

3.2.2. Failure Modes

Post-testing illustrations for all the HAW composites are presented in Figs. 10a-g.

In all cases excluding the specimen made with the BE1 resin (Figure 10b), the LCBC specimens experienced limited cracking within the core matrix/resin, with most of the cracking appearing on the surface of the outer layers. Cracks appear longitudinally and largely localized around different points along the circumference for all four samples, this can be best seen when looking at the cross-section images. In the case of the HAW-EPX-M, the high load capacity has resulted in the crack widening to a point where the outer culm has split into separate pieces, although the crack has not propagated transversely and has remained localized into distinct longitudinal areas. It should be noted that this occurs at very high stresses and near ultimate, which can be evidenced by the composite's high strength values. A similar specimen to HAW-EPX-M with improved hemp wrapping was tested by Mofidi *et al.* [30] which reached a compressive strength of 72.1 MPa.

 doi:10.20944/preprints202407.0293.v1

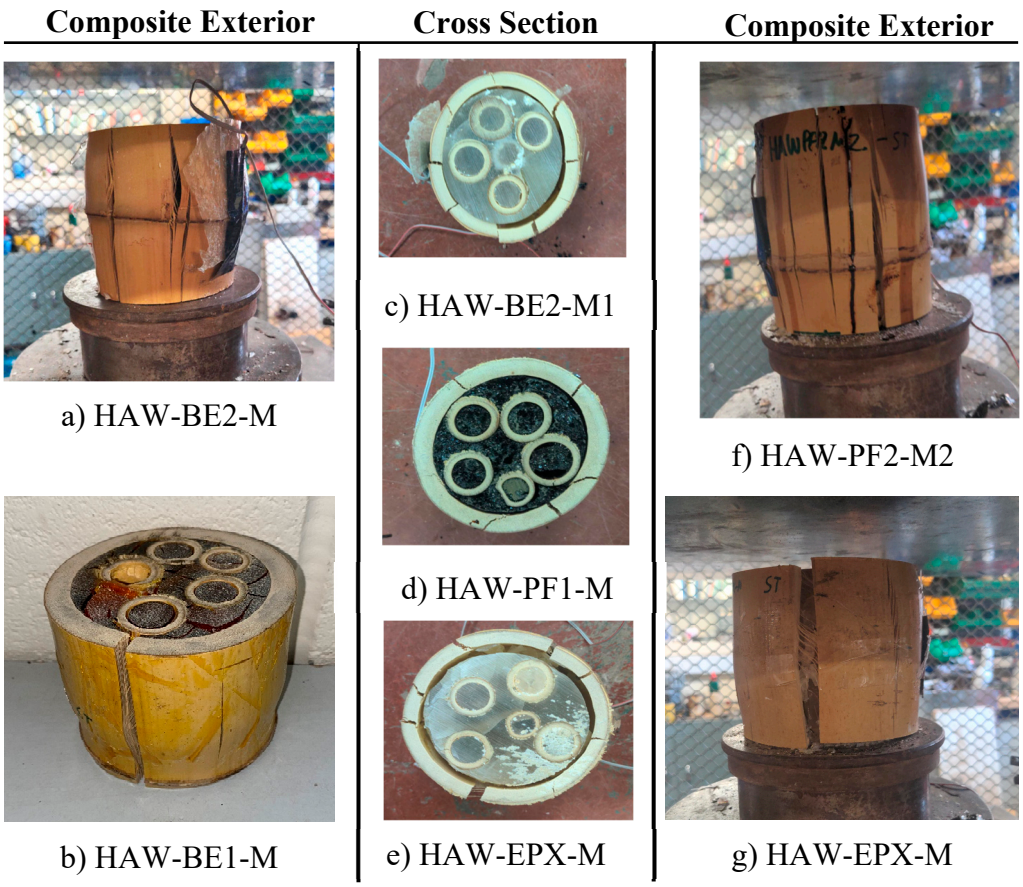

Figure 10. Effect of resin choice on failure modes within HAW specimens.

3.3. Bamboo Species Choice

Compressive Properties

The effect of the bamboo species on the behaviour of the different LCBCs can be observed in the behaviour of specimens in the RD series. Figure 11 reveals the compressive behaviour of specimens with RD configuration and identical resin matrices made with large Moso, Guadua, and Tali species.

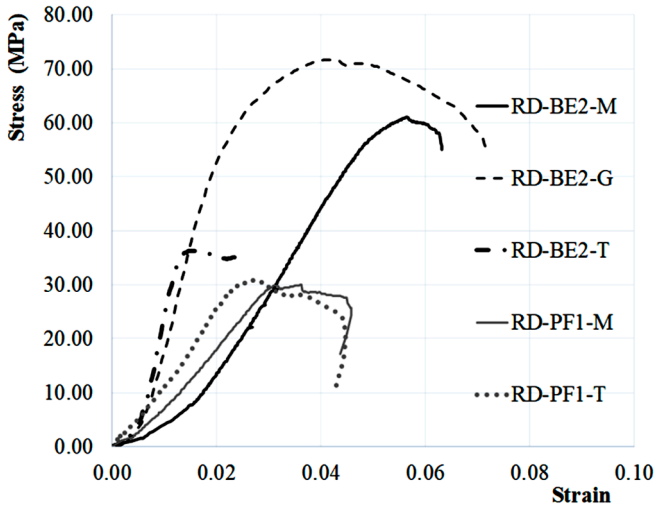

Figure 11. Compressive stress versus measured longitudinal strain of RD test specimens with different bamboo species.

 doi:10.20944/preprints202407.0293.v1

As mentioned earlier, the outer large bamboo acts as the stay-in-place cast when pouring the resin in situ or in the fabrication plant. When comparing the compressive behaviour of RD-BE2-M, RD-BE2-G, and RD-BE2-T specimens, it can be seen that the specimen with Guadua bamboo reached an impressive strength of 72 MPa, followed by the Moso specimen with 61 MPa. The specimen made with Tali bamboo failed prematurely at the compressive stress of 36 MPa due to the splitting of the external bamboo. When it comes to the stiffness of the LCBC made with different species, the stiffest specimen was the LCBC made with Tali species with a modulus of elasticity of 4.47 GPa followed by the Guadua specimen with 3.85 GPa. The specimen made with Moso species reached 1.50 GPa. The stiff compressive behaviour of the Tali LCBC specimens compared to those of Guadua and Moso specimens agrees with the compressive behaviour of raw bamboo used in this study [23]. Such behaviour can also be seen when comparing RD-PF1-M and RD-PF1-T specimens (Figure 11). These specimens are made with PF1 resin which is less stiff compared to BE2 resin. The modulus of elasticity of RD-PF1-M and RD-PF1-T are 1.08 GPa and 1.29 GPa, respectively (Table 3). As reported in [23], the major concern with Tali bamboo is in reliability in terms of consistency in reproducing the same mechanical properties. In terms of the reliability in compressive behaviour the most reliable species is Guadua species as reported in Drury *et al.* [23].

Table 3. Theoretical predictions of the compression tests in HAW series.

Specimen	Theoretical failure strain of first component	Predicted bamboo share (kN)	Predicted resin share (kN)	P_{theory} (kN)	$P_{measured}$ (kN)	$P_{measured}/P_{theory}$
HAW-EPX-M	0.037 (b)*	208.5	313.0	522	568	1.09
HAW-BE1-M	0.037 (b)	292.7	0.1	293	220	0.75
HAW-BE2-M1	0.037 (b)	229.3	188.3	418	398	0.95
HAW-BE2-M2	0.037 (b)	297.2	275.4	573	567	0.99
HAW-BE2-M3	0.037 (b)	216.6	217.4	434	363	0.84
HAW-PF1-M	0.019 (r)	222.1	123.9	346	236	0.68

* Letter (r) or (b) indicate Resin or Bamboo components fail first in each LCBC member, respectively.

4. Theoretical Analysis

The purpose of testing the LCBC components, including resin matrices and bamboo species, was to use principles of composites engineering. The compressive strengths of the LCBC members were predicted through theoretical and numerical analyses. The predictions will be developed to be compared with what was measured from the experimental testing. This will also add some element of validity to the experimental testing methodology carried out in this study. In this regard, the compressive strengths (kN) of the HAW series of LCBC members were calculated in this theoretical analysis.

A two-part equation was used in Mofidi *et al.* [30] on LCBC members which is used here to predict the axial capacity of the HAW LCBC members.

$$P_{theory} = (\sigma_m A_{\mathrm{m}} + \sigma_f A_f) \quad (2)$$

The equation is formed assuming when a composite fails, it is generally due to the failure of one of the components which cascades to the composite as a whole resulting in ultimate failure. The calculated values from the raw bamboo and resin testing can then be applied within this equation. In this equitation, σ_m, A_m, are the compressive strength of the matrix and the area covered by the resin in the LCBC cross-section, respectively. Whereas the compressive strength of fibre (bamboo here) and the area covered by bamboo in the cross-section are σ_f and A_f, respectively. The decision of which component fails first is achieved by calculating the theoretical failure strains of each component. The

 doi:10.20944/preprints202407.0293.v1

component with the smaller ultimate material compressive strain is considered to be the component which fails first and therefore its calculated strength becomes the strength value used in Eq. (2). Similarly, the calculation for the contribution of the second component to the compressive capacity is based on the Hooke's law. Although in this case the ultimate strain of the first component to fail alongside the Youngs Modulus of the second component is used. Table 3 reveals the calculated capacity of the specimens in the HAW test series using Eq. 2.

The mean ratio of the measured compressive capacity ($P_{measured}$) over the predicted compressive capacity (P_{theory}) for all specimens in HAW series is 0.88 with a Coefficient of Variation (CoV) of 16% which indicates reasonable theoretical predictions of the compressive capacities of the tested specimens (Table 3).

5. Finite Element Analysis

5.1. Compressive Behaviour

The present study benefits from a finite element analysis (FEA) software ABAQUS [31] to model the behavior of LCBC short columns in compression. Static Riks analysis is carried out to determine the LCBC response to axial compressive loading. The model in ABAQUS is constructed of full culm Moso bamboo fibres embedded in EPX and BE2 resins and a stay-in-place giant Moso bamboo cast, i.e., HAW-EXP-M and HAW-BE2-M specimens.

The constitutive model of Moso bamboo given as input to ABAQUS (Figure 12) has nonlinear behavior. It demonstrates the point where yielding, plastic deformation, and eventual failure happen (based on experimental data) [32]. The Poisson's ratio is 0.3 [33]. The elasto-plastic behavior of EXP and BE2 resins are used as depicted in Figure 12 [34]. Additionally, the Poisson's ratio is taken as 0.37 [35].

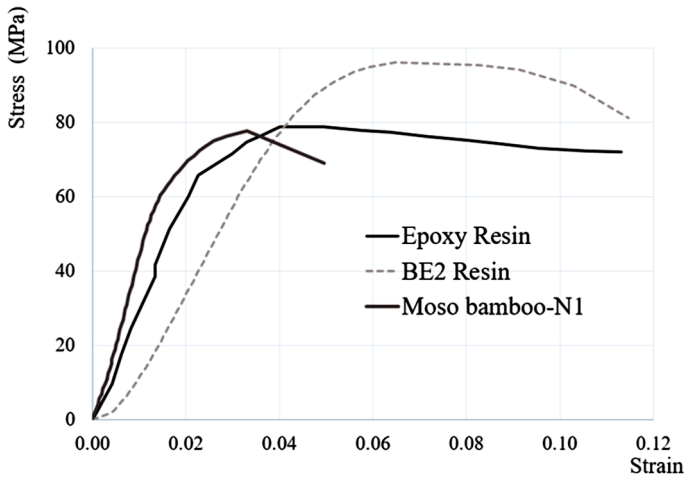

Figure 12. Engineering behavior of Moso bamboo [32] and Resins [34].

The model incorporates isotropic elastic and plastic material behavior for the resins and bamboo. A ductile damage model is utilized for the bamboo and resin matrices. The damage evolution, including fracture strain, stress triaxiality, and strain rate, is measured and incorporated into the model [36]. The bamboo fibres are embedded in resins, and the resin is bonded to the outer bamboo structure by tie constraint [37].

Due to the geometry of the bamboo composite modeled in the present paper, a three-dimensional FEA was carried out. Three dimensional eight-node linear brick elements with reduced integration (C3D8R) are used. For the C3D8R element, hourglass control was included to ensure the element do not get excessively flexible. The literature [38,39] suggests employing 8-node thermally coupled axisymmetric solid elements (CAX8T elements) to model a cylindrical block of resin. However, thermal analysis of the block is excluded in this study, and C3D8R elements are substituted

 doi:10.20944/preprints202407.0293.v1

instead. H-version mesh refinement was used to allow convergence of the outputs given by the FEA [40]. A mesh refinement strategy, based on a sensitivity analysis of mesh sizing, led to the selection of elements with dimensions of 5 mm, enabling finer resolution of the column geometry and ensuring accurate results.

For non-linear analysis of plastic behavior of the Moso bamboo and epoxy, the static-Riks method is applicable [41]. The static-Riks method is better adapted to solve problems where large deformations before buckling can occur. The underlying algorithm used for static-Riks is the Newton-Raphson method, which has been modified to give non-linear static equilibrium solutions to problems that are unstable in nature [42]. The static-Riks method can solve the complicated load-displacement behavior, such as the tangent stiffness changing signs at softening point.

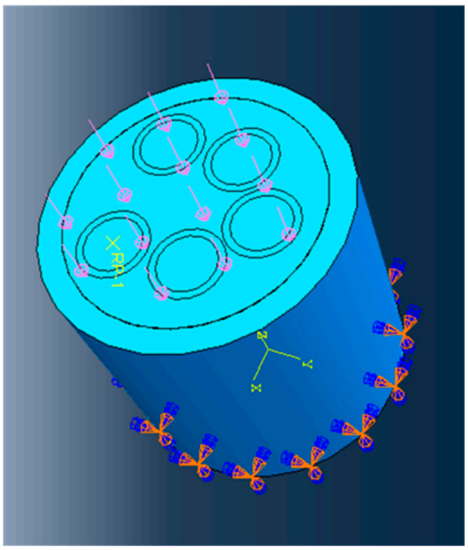

Figure 13. Bamboo composite column model.

For non-linear analysis of plastic behavior of the Moso bamboo and epoxy, the static-Riks method is applicable [41]. The static-Riks method is better adapted to solve problems where large deformations before buckling can occur. The underlying algorithm used for static-Riks is the Newton-Raphson method, which has been modified to give non-linear static equilibrium solutions to problems that are unstable in nature [42]. The static-Riks method can solve the complicated load-displacement behavior, such as the tangent stiffness changing signs at softening point.

In the experimental testing of the HAW-EPX-M, the axial stress at rupture was 77.9 MPa with an axial strain at rupture of 0.044 (Figure 14). The specimen modeled using the C3D8R elements gives results closest to the experimental values, with the axial stress at failure differing by only 2 MPa. The result is 80.3 MPa for the FEA output compared to experimental result of 77.9 MPa. At the point of rupture, the axial strain of the model is 0.046. The load at rupture is 682 kN, and the axial displacement is 4.4 mm.

Preprints.org (www.preprints.org) | NOT PEER-REVIEWED | Posted: 3 July 2024 doi:10.20944/preprints202407.0293.v1

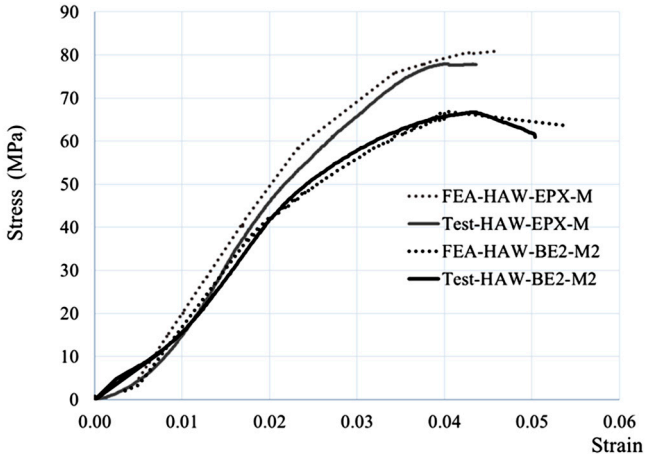

Figure 14. Comparison of compressive stress and measured longitudinal strain of RD test specimens for HAW configuration versus Finite Element Analysis (FEA) results.

For showing the area with the largest stress concentration, the Mises stress is compared in each of the parts of the composite. It can be observed that the stress distribution correlates with the failure mode of the physical specimen (Figure 15a).

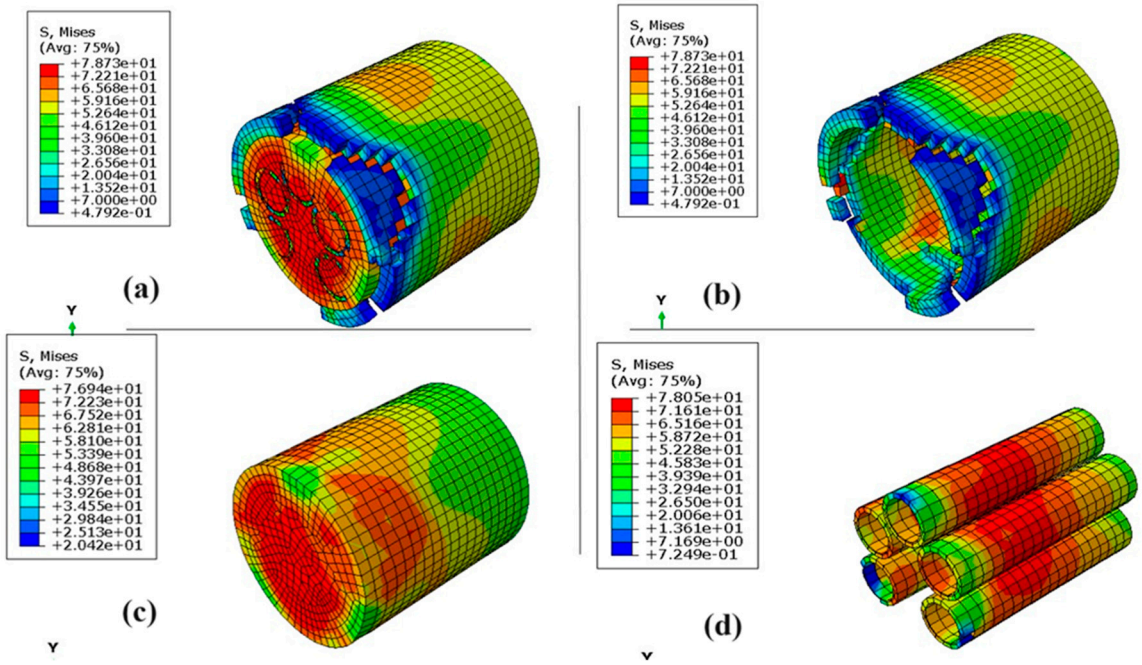

Figure 15. Mises stress distribution of (a) HAW-EPX-M column, (b) Outer bamboo culm, (c) the epoxy matrix, and (d) Bamboo fibres.

High stresses can be visualized throughout the outer bamboo culm, with the failed element throughout the part (Figure 15b). Most of the cracking appears on the surface of the outer layers, mirroring the observed test results. The stress distribution is more complex and variable in matrix (Figure 15c). A stress concentration can be visualized at the base of the specimen. An additional location that experiences a large stress concentration is close to the midspan, where large lateral displacements of the column occur (Figure 15b). The bamboo fibres have undergone high stress, leading to failure in certain elements (Figure 15d). The bamboo fibres have failed primarily at the upper sections of the culms where the load was applied. This area corresponds to the part of the fibre that undergoes large lateral displacements under loading. The failure mode observed in real cases confirms that the bamboo fibres have indeed failed at the upper sections of the culms. Referenced in

 doi:10.20944/preprints202407.0293.v1

literature [23], techniques like wrapping hemp around compressed elements minimize stress in bamboo fibers compared to other constitutive parts.

When comparing the experimental testing of the HAW-BE2-M2, there is a difference of 3 MPa in the axial stress at failure. The FEA output indicates a result of 64 MPa, whereas the experimental result is 67 MPa. At the point of failure, the axial strain measures 0.054, which is close to the experimental value of 0.043. The load at failure, displacements, and stress-strain graphs obtained by the FEA are comparable to the experimental findings, with only minor differences observed. The results are compared to empirical findings, giving insights into the quality of experimental results. This also allowed for an evaluation of the methods and assumptions applied in the model.

5.2. Resin Content Rate Effect

Resin content rate is crucial in composites as it directly influences their mechanical properties and durability. Acting as the bonding agent, resin binds reinforcing fibers, impacting strength, stiffness, weight, and resistance to environmental factors. Achieving the right resin amount is vital to ensuring optimal performance across diverse applications. Enhancing control over resin content is crucial for maintaining consistency and quality in manufacturing processes. To delve deeper into this aspect, a parametric study has been undertaken. This study aims to illuminate the effects of enlarging the outer column dimensions while keeping the outer bamboo wall thickness consistent. By doing so, it investigates how these alterations influence the cross-sectional areas achieved and subsequently impact resin content rate within the composite.

Figures 16 and 17 presents the stress-strain graphs from the parametric investigations focusing on the cross-sectional area of HAW-EPX and HAW-BE2 columns. These figures highlight variations in cross-sectional areas achieved by enlarging the outer column dimensions while maintaining consistent the outer bamboo wall thickness, thereby inducing changes in resin content rate. The cross-sectional areas are systematically adjusted relative to the current section, varying at ratios of 1.2, 1.1, 1, 0.9, and 0.8. In the simulated cases, the configuration denoted by resin content labeled as FEA-A1 showcases the maximum resin content when the cross-sectional area is scaled to 1.2 times the current section's area. The index, ranging from FEA-A1 to A5, correlates with the extent of variation between maximum and minimum cross-sectional areas.

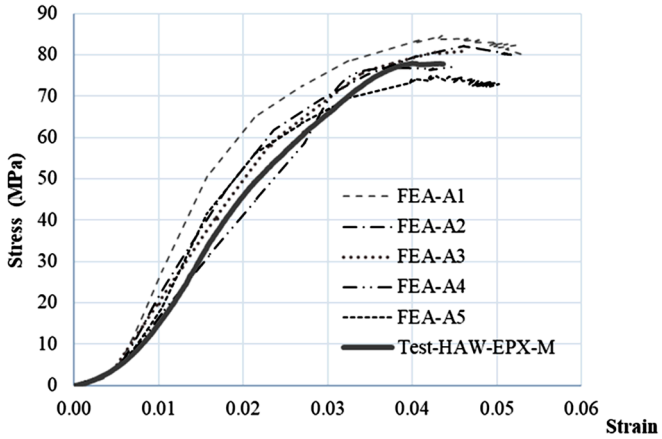

Figure 16. Parametric FEA on compressive stress and measured longitudinal strain in HAW-EPX-M, alongside experimental results.

The extracted data from Figure 16 are presented in Table 4. The overall idealized radius of the column is denoted as *r*.

 doi:10.20944/preprints202407.0293.v1

Table 4. The data extracted from the parametric study of stress-strain curves of HAW-EPX-M under compression load (Figure 16).

Property/Specimen name	FEA-A1	FEA-A2	FEA-A3	FEA-A4	FEA-A5
Radius of section (R_S)	1.2r	1.1r	r	0.9r	0.8r
Peak stress (S_P), MPa	83.7	82.1	80.6	78	74.96
Stress at failure (S_F), MPa	79.3	80.0	79.5	77.2	73.69
Degree of Stress softening (S_P - S_F), MPa	4.40	2.11	1.10	0.80	0.65
Strain at peak (ε_P)	0.040	0.050	0.043	0.033	0.043
Strain at failure (ε_F)	0.050	0.052	0.046	0.045	0.05
Strain gradient at softening (ε_F - ε_P)	0.010	0.002	0.003	0.012	0.007
Stiffness (E_0), GPa	3.70	2.94	2.55	2.49	2.30

A discernible trend is observed wherein the peak stress (SP) which reduces gradually with increasing resin content. The disparity between stresses corresponding to A1 and A5 of the cross-sectional area is reported as 12%.

The phenomenon of softening subsequent to peak stress (SP), akin to necking in ductile materials, is universally observed across all instances examined. The degree of softening can be measured by analyzing the variance between the peak stress level (SP) and stress at failure (SR). Among the simulated cases, A5 with the minimum resin content shows the least degree of softening. This indicates a comparatively faster progression towards failure in this particular configuration relative to others. The strain gradient for this case is 0.007.

Additionally, the initial stiffness of the column, reflected by the gradient of the initial linear segment, decreases with decreasing the resin content, as elucidated in Table 4. It is noteworthy that the reduction in stiffness with resin content can be theoretically verified from the rule of mixture. The reduction observed between column A1 and A5 is precisely 50%.

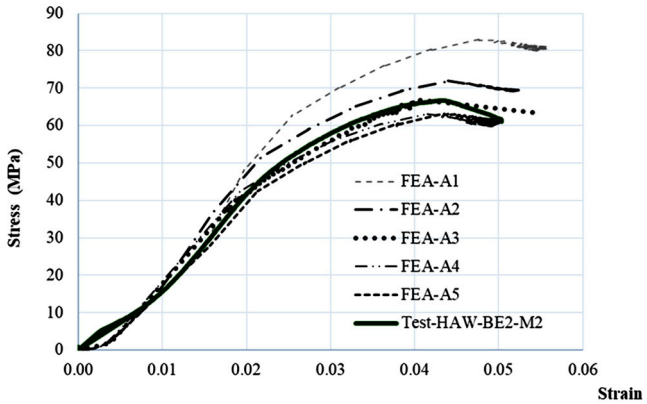

Figure 17. Parametric FEA on compressive stress and measured longitudinal strain in HAW-BE2-M2, alongside experimental results.

Table 5 presents the findings extracted from the parametric study on the FEA models based on HAW-BE2 specimen. A comparative analysis between the results delineated in the two tables leads

 doi:10.20944/preprints202407.0293.v1

to the following conclusions on the effect of the resin content on the behaviour of the studied specimens:

- The reduction in stiffness observed in columns employing BE2 is less pronounced compared to those utilizing an EPX matrix, attributable to the inherently greater stiffness of EPX.
- The degree of Stress softening, defined as the difference between the maximum stress and the failure stress, exhibits negligible variation across the five cases examined.
- The difference in peak stress levels between sections A1 and A2 is more pronounced in columns using BE2 materials than those using EPX.

Table 5. The data extracted from the parametric study of stress-strain curves of HAW-EPX-M under compression load.

Property/Specimen name	**FEA-A1**	**FEA-A2**	**FEA-A3**	**FEA-A4**	**FEA-A5**
Radius of section (R_S)	1.2r	1.1r	r	0.9r	0.8r
Peak stress (S_P), MPa	82.95	71.93	66.90	63.05	63.15
Stress at failure (S_F), MPa	80.45	69.28	63.50	60.41	61.50
Degree of Stress softening (S_P - S_F), MPa	2.50	2.65	3.40	2.64	1.65
Strain at peak (ε_P)	0.048	0.044	0.04	0.042	0.044
Strain at failure (ε_F)	0.056	0.053	0.054	0.047	0.050
Strain gradient at softening (ε_F - ε_P)	0.008	0.009	0.014	0.005	0.006
Stiffness (E_0), GPa	2.70	2.20	1.94	1.65	1.55

6. Conclusions

In this study, 17 Low-Cost Bamboo Composite (LCBC) short columns have been investigated experimentally, numerically, and theoretically. The principal testing parameter of this investigation is the cross-sectional configurations, in addition to the choices of bio-resin matrices and bamboo species. Four different cross-sectional configurations, including HAW, BRD, RD, and SCR were proposed to be used with bio-epoxy (BE2), furan-based resin (PF1), and synthetic epoxy (EPX) resin. From the outcomes of this study the following conclusions can be drawn:

- Unprecedented LCBC compressive members with bio-based resins were able to reach a massive compressive capacity of 567 kN for a member with 104.1 mm diameter which corresponds to 67 MPa (HAW-BE2-M);
- The maximum compressive strengths (MPa) achieved by two specimens with synthetic epoxy closely followed by a specimen with bio-epoxy namely HAW-EPX-M, RD-EPX-M, and RD-BE2-G specimens with 78 MPa, 75 MPa, and 72 MPa, respectively;
- The most efficient cross-sectional configurations with respect to the compressive strength and modulus of elasticity were the HAW configuration followed by the SCR configuration based on the outputs of tests on two different bio-resins;
- The BRD cross-sectional configuration, with greater bamboo content compared to the rest of the proposed configurations, is the most efficient configuration when used with a resin weaker than bamboo in compression such as PF1;
- In terms of the modulus of elasticity of LCBC with different resin matrices, the stiffest specimens are HAW-BE2-M1, HAW-EPX-M, and HAW-BE2-M2 with 3.89 GPa, 3.08 GPa, and 2.54 GPa;

- The specimen made with furan-based resin was able to contribute significantly to the stiffness of the LCBC with a modulus of elasticity of 2.06 GPa when compared to the HAW-BE1-Mcontrol specimen with a soft matrix;
- When assessing the effect of the stay-in-place choice of bamboo species, the specimen with Guadua bamboo reached an impressive strength of 72 MPa, followed by the Moso specimen with 61 MPa while the specimen with Tali species reached the greatest modulus of elasticity with 4.47 GPa (the greatest among all 17 specimens) but failed prematurely at 36 MPa;
- The theoretical predictions of the specimens in HAW series reached a reasonable accuracy with Mean value equal to 0.88 and CoV equal to 16% for the $P_{measured}/P_{theory}$ ratio;
- FEA conducted with ABAQUS effectively simulates the response of the LCBC columns with HAW configuration to axial compression. The numerical model integrates constitutive models for Moso bamboo and epoxy resins. Mesh refinement strategies, with elements of 5 mm, ensure convergence and accuracy.
- The numerical analysis output closely matches experimental results, with only minor differences observed, such as a 2 MPa difference for axial stress at failure in HAW-EPX-M specimens and a 3 MPa difference in HAW-BE2-M2 specimens.
- Resin content profoundly affects composite properties like strength and stiffness, emphasizing the need for precise control during manufacturing. Parametric studies show that adjusting outer column dimensions while keeping wall thickness consistent alters resin content, peak stress, and stiffness. A discernible trend is observed wherein the peak stress (SP) reduces gradually with increasing resin content. Additionally, the initial stiffness of the column decreases with decreasing the resin content, particularly up to a 50% reduction.
- The consistency between experimental data and simulated results bolsters the confidence in the predictive capacity of the model. The stress-strain behavior graphs and observed failure mode during simulation demonstrate the accuracy of the model.

Author Contributions: Conceptualization, A.M. and G.S.; methodology, A.M and G.S.; software, G.S. and M.R.; validation, G.S., M.R. and A.M.; formal analysis, A.M. and G.S.; investigation, C.P., B.D., G.S. and A.M; resources, A.M.; data curation, M.R. and A.M.; writing—original draft preparation, A.M., G.S., C.P. and B.D.; writing—review and editing, A.M. and G.S.; visualization, A.M. and G.S.; supervision, A.M.; project administration, A.M.; funding acquisition, A.M. All authors have read and agreed to the published version of the manuscript.

Funding: This research was partially supported by NSERC Discovery Grant RGPIN 2023-05246 to Dr. Mofidi.

Data Availability Statement: No new data was created or analyzed in this study. Data sharing is not applicable to this article,

Conflicts of Interest: The authors declare no conflicts of interest.

Acknowledgement: The financial support of the National Science and Engineering Research Council of Canada, through operating grants to Dr. Amir Mofidi to cover the analytical and numerical research team salaries is gratefully acknowledged. The authors thank Dr Jean Hall for her continuous support of M.Eng. research at Newcastle University. The efficient collaboration of Stuart Patterson (engineering laboratory team leader), Gareth Wear (senior laboratory technician) and Michael Finlay (heavy structures laboratory technician) at Newcastle University in conducting the tests is acknowledged. The authors acknowledge Transfurans Chemicals BVBA valuable and generous donation of Biorez 141010 and technical support on the resin application.

References

1. Javadian A, Wielopolski M, Smith IFC, Hebel DE. Bond-behavior study of newly developed bamboo-composite reinforcement in concrete. *Construction and Building Materials Journal*. **2016**, *122*, 110-117.
2. Arioğlu Akan, M.Ö, Dhavale, D.G, Sarkis, J Greenhouse gas emissions in the construction industry: An analysis and evaluation of a concrete supply chain. *Journal of Cleaner Production*, **2017**, *167*, 1195–1207.
3. Rodrigues, F, Joekes, I Cement industry: sustainability, challenges and perspectives. *Environmental Chemistry Letters*, **2010**, *9(2)*, 151–166.

4. World Steel Association Steel's contribution to a low-carbon future and climate resilient societies. *World Steel Association* **2020**, Report. No. 6.
5. Birol, F, Solheim, E Global Status Report 2017: Towards a zero-emission, efficient, and resilient buildings and construction sector. *United Nations Environment* **2017**, 48 pages.
6. Khatib, J.M Sustainability of construction materials, 2nd edition; *Woodhead Publishing*, **2016**, 742 pages.
7. Richardson, C, Mofidi, A Non-Linear Numerical Modelling of Sustainable Advanced Composite Columns Made from Bamboo Culms, *Construction Materials* **2021**, *1(3)*, 169-187.
8. van der Lugt, P. (Design Interventions for Stimulating Bamboo Commercialization: Dutch Design Meets Bamboo as a Replicable Model. Ph.D. Thesis, Delft University of Technology **2008**, Delft, The Netherlands.
9. Shu, B, Xiao, Z, Hong, L, Zhang, S, Li, C, Fu, N, Lu, X Review on the application of bamboo-based materials in construction engineering, *Journal of Renewable Materials* **2020** *8(10)*, 1215–1242.
10. Trujillo, D.J.A, Malkowska, D Empirically derived connection design properties for Guadua bamboo, *Construction and Building Materials* **2018** *163*, 9-20.
11. Koenigsberger, O.H World consultation on the use of wood in housing: Wood in housing in developing countries (Section 6) Unasylva Journal of Food and Agriculture Organization of the United Nations **1971** *25* 101-103.
12. Harries, K.A, Sharma, B, Richard, M. Structural Use of Full Culm Bamboo: The Path to Standardization. International Journal of Architecture, *Engineering and Construction*, **2012** *1(2)*, 66–75.
13. Bhagat, D, Maheshwari, A, Bhalla, S. Composite bamboo beam elements for structural applications. *In Proceedings of UK-India Education and Research Initiative (UKIERI) Congress on Innovations in Concrete Construction*, Jalandhar, India, (05 August 2013).
14. Nunes, N. Nonwood bio-based materials in: Performance of Bio-based Building Materials, *Woodhead Publishing* **2017** 97–186.
15. Kaminski, S.; Lawrence, A.; Trujillo, D. Structural use of bamboo. Part 1: Introduction to bamboo. *The Structural Engineer* **2016** *98(8)*, 40–43.
16. Trujillo, D. and López, L.F Bamboo material characterisation. In Nonconventional and Vernacular Construction Materials, 2nd *Woodhead Publishing* **2016**, 365–392.
17. Harries, K.A, Mofidi, A, Naylor, J, Trujillo, D.J.A, Gutierrez, M and Sharma, B Knowledge Gaps and Research Needs for Bamboo in Construction. *The 18th International Conference on Non-conventional Materials and Technologies*. (07 July 2022).
18. Nurdiah, E.A The Potential of Bamboo as Building Material in Organic Shaped Buildings *Procedia - Social and Behavioral Sciences*, **2016** *216*, 30–38.
19. Mofidi, A, Abila, J, and Ng, J.T.M Novel Advanced Composite Bamboo Structural Members with Bio-Based and Synthetic Matrices for Sustainable Construction, *Sustainability* **2020**, *12*, 2485.
20. Maiti, S, Islam, R, Uddin, M.A, Afroj, S, Eichhorn, S.J, Karim, N Sustainable Fibre-Reinforced Composites: A Review, *Advanced Sustainable Systems*, **2022** *6(11)*, 2200258.
21. ISO 22157:2019 Bamboo structures - Determination of Physical and Mechanical Properties of Bamboo Culms – Test Methods. *International Standards Organization*, **2019** 25 Pages.
22. Drury, B, Padfield, C, Russo, M, Swygart, L, Spalton O, Froggatt, S, and Mofidi, A. Assessment of the Compression Properties of Different Giant Bamboo Species for Sustainable Construction. *Sustainability* **2023** *15(8)*:10.3390/su15086472.
23. Trujillo, D.J, López, L.F Bamboo material characterisation in Nonconventional and Vernacular Construction Materials (Second Edition): Characterisation, Properties and Applications, *Woodhead Publishing* **2020** Pages 491-520.
24. Kenneth, O.I and Uzodimma, U.O Evaluation of the Compressive Strength of Bamboo Culms under Node and Internode Conditions, *Saudi J Civ Eng*, **2021** *5(8)*, 251–258.
25. Klose, L, Meyer-Heydecke, N, Wongwattanarat, S, Chow, J, Pérez García, P, Carré, C, Streit, W, Antranikian, G, Romero, AM, Liese, A. Towards Sustainable Recycling of Epoxy-Based Polymers: Approaches and Challenges of Epoxy Biodegradation. *Polymers*. **2023** *15(12)*:2653:10.3390/polym15122653.
26. Terry, J.S, and Taylor, A.C The properties and suitability of commercial bio-based epoxies for use in fiberfibre-reinforced composites, *Journal of Applied Polymer Science*, **2021** *138(2)*: 10.1002/app.50417.
27. Ferdosian, F, Zhang, Y, Yuan, Z, Anderson, M, and Xu CC. Curing kinetics and mechanical properties of bio-based epoxy composites comprising lignin-based epoxy resins, *European Polymer Journal*, **2016** *82*, 153-165.

 doi:10.20944/preprints202407.0293.v1

28. Hoydonckx, H.E, Van Rhijn, Wim Application of novel furan resins in composites, *JEC Composites Magazine*, **2008** *45(38)*, 34-35.
29. ASTM D695 (. Standard Test Method for Compressive Properties of Rigid Plastics. *American Society for Testing and Materials*, **2015**, West Conshohocken, Pennsylvania, United States.
30. ABAQUS. Abaqus Unified FEA-3DEXPERIENCE R2018; Systèmes, D., Ed.; 3DS-SIMULIA: Rue Marcel Dassault, Vélizy-Villacoublay, France, **2018**.